Articles

Structure and Function of the Virulence-Associated High-Temperature Requirement A of *Mycobacterium tuberculosis*[†,‡]

Nilofar N. MohamedMohaideen,[§,△] Satheesh K. Palaninathan,[§,△] Paul M. Morin,[⊥] Brad J. Williams,[#] Miriam Braunstein,[+] Shane E. Tichy,[#] Joseph Locker,[◆] David H. Russell,[#] William R. Jacobs, Jr.,[▽] and James C. Sacchettini*[,§]

Department of Biochemistry and Biophysics, Texas A&M University, College Station, Texas 77843, Department of Chemistry, Texas A&M University, College Station, Texas 77842, Howard Hughes Medical Institute, Department of Microbiology and Immunology, Albert Einstein College of Medicine, Bronx, New York 10461, U.S. Food and Drug Administration, Microbiological Sciences Branch, Jamaica, New York 11433, Department of Microbiology and Immunology, University of North Carolina, Chapel Hill, North Carolina 27599, and Department of Pathology, Albert Einstein College of Medicine, Bronx, New York 10461

Received September 21, 2007; Revised Manuscript Received December 7, 2007

ABSTRACT: The high-temperature requirement A (HtrA) family of serine proteases has been shown to play an important role in the environmental and cellular stress damage control system in *Escherichia coli*. *Mycobacterium tuberculosis* (*Mtb*) has three putative HtrA-like proteases, HtrA1, HtrA2, and HtrA3. The deletion of *htrA2* gives attenuated virulence in a mouse model of TB. Biochemical analysis reveals that HtrA2 can function both as a protease and as a chaperone. The three-dimensional structure of HtrA2 determined at 2.0 Å resolution shows that the protease domains form the central core of the trimer and the PDZ domains extend to the periphery. Unlike *E. coli* DegS and DegP, the protease is naturally active due to the formation of the serine protease-like catalytic triad and its uniquely designed oxyanion hole. Both protease and PDZ binding pockets of each HtrA2 molecule are occupied by autoproteolytic peptide products and reveal clues for a novel autoregulatory mechanism that might have significant importance in HtrA-associated virulence of *Mtb*.

Bacterial survival in environmental extremes, including high temperature and oxidative stress, depends on the activities of periplasmic proteases and chaperones (*1–7*). The HtrA[1] proteins are comprised of a family of periplasmic heat shock proteins with both protease and chaperone activity (*5–10*). HtrA proteins have been identified in many organisms, from *Archaea* to humans. Members of this protein family all share a highly conserved serine protease domain containing an active site catalytic triad (Ser-His-Asp) and one or more C-terminal PDZ domains (*9, 10*). PDZ domains are protein modules that mediate specific protein–protein interactions and usually bind three or four C-terminal residues of the target protein (*11–14*). Accumulated evidence indicates that the PDZ domains can both positively and negatively regulate the protease activity of HtrA proteins (*15–17*).

HtrA proteases play important roles in the periplasmic space of *Escherichia coli* as part of the stress response system involving the Cpx two-component system (*18, 19*) and σE pathway (*17, 20*). For example, DegP is part of *E. coli*'s extracytoplasmic stress response system and acts on several misfolded native gene products, including alkaline phosphatase (PhoA) (*21*), DsbA (*22*), and maltose-binding protein variants MalS and MalE (*4, 8, 23*). The diversity of substrates implies that DegP plays a central role in the stability and turnover of periplasmic proteins. DegS and DegQ are two other HtrA enzymes found in *E. coli*. DegS senses the stress

[†] This work was supported by grants from the National Institutes of Health (AIO68135 to J.C.S., AI26170 to W.R.J., and F32-AI149675 to P.M.M.). J.C.S. acknowledges Robert A. Welch Foundation Grant A-0015.

[‡] The atomic coordinates of the mHtrA2 crystal structure have been deposited in the Protein Data Bank as entry 2Z9I.

* To whom correspondence should be addressed. J.C.S.: Department of Biochemistry and Biophysics, Texas A&M University, College Station, TX 77843; telephone, (979) 862-7636; fax, (979) 862-7638; e-mail, sacchett@tamu.edu. W.R.J.: Howard Hughes Medical Institute, Department of Microbiology and Immunology, Albert Einstein College of Medicine, Bronx, NY 10461; telephone, (718) 430-2888; fax, (718) 518-0366; e-mail, jacobsw@hhmi.org.

[§] Department of Biochemistry and Biophysics, Texas A&M University.

[△] These authors contributed equally to this work.

[⊥] U.S. Food and Drug Administration.

[#] Department of Chemistry, Texas A&M University.

[+] University of North Carolina.

[◆] Department of Pathology, Albert Einstein College of Medicine.

[▽] Department of Microbiology and Immunology, Albert Einstein College of Medicine.

[1] Abbreviations: HtrA, high-temperature requirement A; CS, citrate synthase; *Mtb*, *Mycobacterium tuberculosis*; MAD, multiwavelength anomalous diffraction; Δtm-HtrA2, truncated HtrA2; mHtrA2, 32 kDa autolytic product of Δtm-HtrA2; Δtm-S317A-HtrA2, S317A mutant of Δtm-HtrA2; mHtrA2-PDZ, 10 kDa autolytic product of Δtm-HtrA2; rmsd, root-mean-square deviation; Δ*htrA2*, deletion of the *htrA2* gene; SDS, sodium dodecyl sulfate; sigE, sigma factor (E); sigB, sigma factor (B); DegP, Do protease P; DegS, Do protease S; DegQ, Do protease Q; MprA or MprB, *Mycobacterium* persistence regulator A or B, respectively; CpxA, conjugation plasmid expression A; CpxR, conjugation plasmid expression regulator; DsbA, thiol−disulfide interchange protein; MalS or MalE, maltose binding protein S or E, respectively; CFU, colony-forming unit.

10.1021/bi701929m CCC: $40.75
Published on Web 05/15/2008

and triggers the σE stress response pathway (*17, 20, 24*), while the specific role of DegQ is not yet known.

HtrA homologues have also been found in many Gram-positive bacteria and are shown to be important in virulence (*25–28*). However, the functions of these proteins in Gram-positive bacteria remain unclear. Homologues of HtrA are also present in mycobacteria, which are related to Gram-positive bacteria yet have many Gram-negative characteristics, including a periplasmic space (*29*). The genome of *Mtb* contains three genes that encode HtrA serine proteases: *Rv1223* (*htrA1*), *Rv0983* (*htrA2*), and *Rv0125* (*htrA3*). The predicted amino-terminal transmembrane region suggests that, like the *E. coli* HtrA proteins, all three *Mtb* enzymes are localized to the outer leaflet of the membrane in the periplasmic compartment. This correlates well with a previous study that demonstrated that HtrA1 is an integral membrane protein of 55 kDa (*30*). However, the presence of HtrA2 and HtrA3 in the culture medium of cells grown in vitro suggests that these enzymes may be exported to the periplasm (*31–33*). HtrA2 is part of an operon consisting of *mprA(Rv0981)-mprB(Rv0982)-htrA2(Rv0983)-(unknown)-Rv0984*. MprA−MprB is a two-component system required by *Mtb* for growth in vivo during the persistent stage of infection (*34*). Recent studies have also demonstrated that MprA regulates the expression of numerous stress responsive genes in *Mtb*, including *sigB* and *sigE*, while MprB acts as a cognate sensor kinase (*35*). Interestingly, it has been shown that MprA regulates its own expression, as well as the expression level of HtrA2, by binding to the 8 bp conserved motif found upstream of *htrA2* and *mprA* (*36*).

All three *Mtb* HtrA homologues exhibit moderate levels of sequence homology among themselves (32–40% identical) and levels of sequence identity similar to those of the *E. coli* periplasmic proteases DegP, DegS, and DegQ. DegP and DegQ have two PDZ domains, and DegS has a single PDZ domain. The four HtrA homologues identified in the human genome and the three HtrA enzymes of *Mtb* contain only one PDZ domain. However, the function of *Mtb*-HtrA and its specific role in *Mtb* have not yet been explored. Here in this study, we have determined the three-dimensional structure of *Mtb*-HtrA2 and demonstrated that this enzyme is required for the virulence of *Mtb* in mice and that it behaves as both a protease and a chaperone. Our studies show that mHtrA2 undergoes autolytic processing and produces several peptide products; two of these peptides are identified in the PDZ and protease binding pockets of the mHtrA2 crystal structure. Binding of both the peptides to the mHtrA2 active site and PDZ domain suggests that autoproteolysis of this enzyme might be involved in modulating its activity. In addition, we have shown an unusual occurrence of hydrophobic residue clusters associated with the autolytic sites of *Mtb*-HtrA2.

EXPERIMENTAL PROCEDURES

Deletion of the Mtb htrA2 Gene. Flanking DNA sequences of *Mtb-htrA2* were amplified by polymerase chain reaction (PCR) and cloned into vector pJSC284 upstream and downstream of the hygromycin resistance gene. The deletion allele was packaged into a temperature sensitive mycobacteriophage, phAE159, and then packaged into a λ phage. *E. coli* HB101 was transduced with the λ phage, and hygromycin resistant clones were chosen for cosmid isolation. *Mycobacterium smegmatis* was transformed with pooled cosmids, where high-titer phage lysates were obtained for transducing *Mtb* (*37–39*).

Mouse Virulence Experiments. BALB/c SCID and C57BL/6 mice were infected intravenously with 1×10^6 CFU of mycobacteria. Four mice from each experimental group were sacrificed 24 h and 3, 8, and 15 weeks after infection. Organs were analyzed for bacterial burden and histology. A log rank test was used for analyzing the significance of mouse survival, and a statistical hypothesis test (Student's *t*-test) was used to analyze the colony's transformation of units in organs.

Cloning and Purification. The truncated form of *Mtb*-HtrA2 (Δtm-HtrA2) containing residues 125–464 was amplified by PCR from *Mtb*H37Rv genomic DNA. This expression construct contained 31 vector-derived amino acids fused at the N- and C-termini, including two His_6 tags. The PCR product was subcloned into the pET28b vector at the *Nde*I and *Xho*I sites and transformed into BL21(DE3) (Novagen). The S317A mutant of Δtm-HtrA2 was prepared using a QuikChange XL site-directed mutagenesis kit (Strategene). Both native and mutant proteins were expressed in *E. coli* at 37 °C. The cells were grown at 37 °C and 200 rpm in LB (Luria broth) medium with kanamycin (final concentration of 50 μg/mL) until the OD_{600} reached 0.6–0.9. The culture was then induced with 1 mM isopropyl 1-thio-β-D-galactopyranoside (IPTG), and the incubation was continued for an additional 2 h at 37 °C. The bacterial cells were harvested by centrifugation at 4000 rpm for 30 min and resuspended in 20 mM Tris-HCl buffer (pH 8.0) containing 0.5 M NaCl and 5 mM imidazole. For Se-Met protein, the pET28b-Δtm-HtrA2 clone was transformed into *E. coli* B834(DE3) (Novagen) Met auxotrophic cells; the cells were grown in M9 minimal medium with all of the 19 standard amino acids, and methionine was substituted with selenomethionine (50 mg/L). A solution of kanamycin (50 μg/mL) was added to the culture, and the cells were grown at 37 °C until the OD_{600} reached 0.5. The culture was then induced at 25 °C with 1 mM IPTG. For all protein preparations, the cells were lysed using a French press, and the cell suspension was centrifuged at 15000 rpm for 40 min. The 0.2 μm membrane-filtered clear supernatant was then loaded onto an Amersham Biosciences Hi-trap Ni^{2+} chelating column that was equilibrated with the cell resuspension buffer, and the protein was eluted using an imidazole gradient [20 mM Tris-HCl buffer (pH 8.0), 0.5 M NaCl, and 200 mM imidazole]. All proteins were purified by a nickel affinity column, followed by size exclusion chromatography using Superose 6 (Amersham Pharmacia). The protein band for the expressed Δtm-HtrA2 appeared at 32 kDa instead of 37 kDa as observed via SDS−PAGE. Along with this 32 kDa protein band, another strongly expressed protein band of approximately 10 kDa was observed in the soluble fraction of the recombinant *E. coli* lysate. This 10 kDa protein (mHtrA2-PDZ hereafter) was copurified using a nickel column and separated using size exclusion chromatography. Attempts to crystallize this 10 kDa protein were unsuccessful. The fractions containing the 32 kDa product of Δtm-HtrA2 (mHtrA2 hereafter) were pooled, concentrated, and crystallized.

Crystallization and Data Collection. Crystals of mHtrA2 were obtained at 16 °C from a solution of 7 mg/mL protein

[in 50 mM Tris-HCl and 1 mM dithiothreitol (DTT) (pH 7.0)], 0.1 M sodium acetate (pH 4.6), 0.1 M cadmium chloride, and 30% PEG 400 using the hanging drop method. mHtrA2 was crystallized in the monoclinic space group. A single crystal was mounted in a cryo-loop and was flash-cooled to 100 K after a brief soak in *N*-paratone oil. X-ray diffraction data sets were collected at synchrotron beamline BioCARS 14-ID-B of the Advanced Photon Source (Argonne National Laboratory, Argonne, IL) and processed with HKL2000 using DENZO and SCALEPACK (*40*).

Structure Determination. Multiwavelength anomalous diffraction (MAD) phasing (*41*) was used with diffraction data collected from a Se-Met mHtrA2 crystal at three different wavelengths. Four (out of nine) Se sites were identified using SHELXD (*42*) and were refined by SHARP (*43*). Solvent flattening SOLOMON (*44, 45*) improved the electron density map to the point where an initial protein model could be constructed using Xtalview (*46*). The asymmetric unit contained three molecules (molecules A, B, and C). The electron density map corresponding to the protease domain (residues 149–364) of each molecule was mostly similar. The PDZ domain of molecule A (residues 376–464) is continuous and well-ordered. In contrast, the PDZ domains of molecules B and C exhibited an increased flexibility and contained a greater number of disordered residues. Disordered protein residues (see Table 1), which are not visible in the electron density map, were omitted from the model; 327 water molecules were identified by Xtalview (*46*) and were included in the refinement. A refined model was produced through several cycles of manual model building and maximum likelihood refinement in CCP4-Refmac5 (*47*). Clear, continuous, and unexplained electron density above the 1σ cutoff in the experimental map was observed in both the protease and PDZ binding pocket of HtrA2 (Figure 1a, b). The additional densities were interpreted as extended polypeptides of VEQV and GATV. Several other equivalent tetrapeptide residues were examined and ruled out by close examination of the interactions of the peptide with the binding pocket. Further refinement after including these peptides yielded the final model with an R_{factor} of 22.5% and an R_{free} of 27.2%. The final model gave good stereochemistry (Table 1) as determined by the Ramachandaran plot [calculated with PROCHECK (*48, 49*)]. The crystal data and refinement statistics are given in Table 1, and the atomic coordinates were deposited in the Protein Data Bank as entry 2Z9I. The figures were prepared using Spock (http://quorum.tamu.edu), Raster3D (*50*), and Chimera (*51*).

Protease Assay. The bovine β-casein (Sigma) was used as a substrate. The assay buffer contained 50 mM sodium cacodylate (pH 7.4), 5 mM $MgCl_2$, and 1 mM DTT. For 2 h, 5–10 μg of mHtrA2 was incubated with 70 μg of β-casein at 37 °C in a total reaction volume of 80 μL. The results were analyzed by SDS−PAGE, and the products were stained with Coomassie brilliant blue (Figure 2a).

Chaperone Assay. The chaperone-like activities of mHtrA2, the S317A mutant of Δtm-HtrA2, and the 10 kDa product of HtrA2 (mHtrA2-PDZ) were measured using pig heart citrate synthase (CS) as the substrate as described previously (*52–54*). CS (Sigma) was denatured in a solution containing 100 mM Tris-HCl (pH 8.0), 100 mM NaCl, 6 M guanidinium hydrochloride, and 40 mM DTT for 2 h at room temperature.

Table 1: Crystal Data and Refinement Statistics

Data Collection Statistics			
	Se-Met mHtrA2		
wavelength (Å)	0.97900	0.97923	0.94181
data set	peak	inflection	high remote
resolution (Å)	77.0–1.86	50.0–2.10	50.0–2.10
completeness (%) (last shell)	93.8 (72.1)	93.6 (71.8)	91.2 (64.9)
$I/\sigma(I)$ (last shell)	24 (0.9)	16.2 (1.0)	12.3 (0.8)
no. of unique reflections	73413	49525	48158
R_{sym} (%)	5.3	7.4	9.9

Refinement Statistics	
unit cell dimensions	a = 149.6 Å, b = 89.1 Å, c = 69.4 Å, β = 97.5°
space group	*C*2
no. of protomers per asymmetric unit (*Z*)	3
no. of reflections in the working set	57235
no. of reflections in the test set	3078
completeness (%)	98.8
R_{factor} (%)	22.5
R_{free} (%)	27.2
no. of protein residues	827
no. of solvent molecules	327
disordered residues	molecule A: 149–153, 175–178, 205–210, 293–299, 339–345, 463–472 molecule B: 149–151, 174–177, 204–211, 293–299, 339–345, 387–390, 399–401, 445–454, 464–472 molecule C: 149–153, 174–177, 293–298, 339–346, 386–389, 398–400, 404–407, 441–458, 463–472
average *B* factor for protein (Å^2)	43.7 (molecule A), 48.9 (molecule B), 49.5 (molecule C)
average *B* factor for water (Å^2)	47.2
rmsd for bond lengths (Å)	0.009
rmsd for bond angles (deg)	1.6
Ramachandran statistics	
most favored (%)	92
allowed (%)	8

The denatured CS was diluted 200-fold into a refolding buffer containing 10 mM Tris-HCl (pH 8.0) and enzyme to reach the required molar ratios (Figure 2b). The change in turbidity caused by the aggregated proteins was monitored by measuring the absorbance at 320 nm with a Cary 100 spectrophotometer at room temperature.

MALDI-MS Analysis. Linear mode matrix-assisted laser desorption ionization (MALDI) time-of-flight mass spectrometry (MS) data were acquired using a Voyager DE-STR instrument (Applied Biosystems, Foster City, CA) under optimized conditions. The HtrA2 sample was diluted 10-fold in ddH_2O and mixed 1:1 with MALDI matrix [15 mg/mL sinapic acid (Sigma-Aldrich, St. Louis, MO) and 50:50 acetonitrile (ACN)/ddH_2O mixture with 0.1% trifluoroacetic acid (TFA)].

LC−MALDI-MS/MS Analysis. Crystals of mHtrA2 were resuspended in 300 μL of 10 mM Tris-HCl buffer at pH 7.5. The protein solution was allowed to undergo autolytic digestion at 10 °C. The protein solution was diluted 10-fold in ddH_2O and filtered through a 10 kDa MWCO filter (Millipore, Bedford, MA) to remove the intact protein. The resulting solution was then subjected to liquid chromatography−mass spectrometry (LC−MS) analysis by injecting

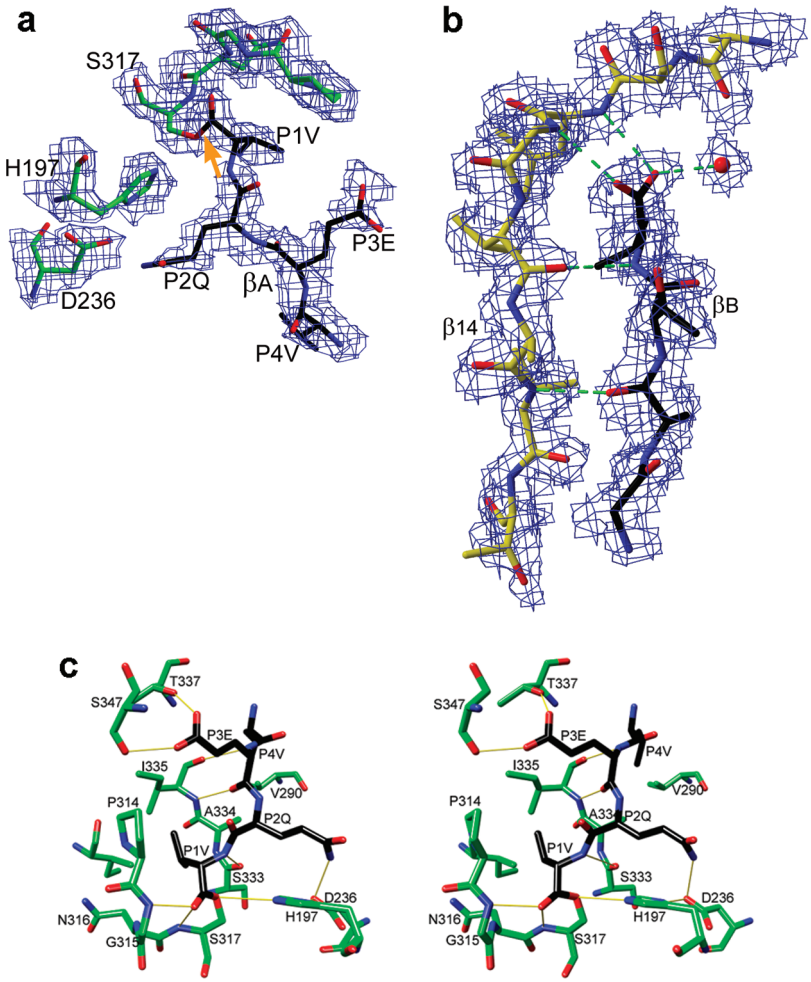

FIGURE 1: (a) Electron density map showing the covalently bound tetrapeptide βA in the protease binding pocket (the arrow points to the acyl−Ser317 covalent linkage). The 2.0 Å resolution map (contoured at the 1σ level) was the result of experimental MAD phasing. The "blob" feature in XTALVIEW has been applied to limit the electron density display within 1.5 Å of the residues. (b) Experimental electron density map (contoured at the 1σ level) showing the tetrapeptide βB bound in the PDZ domain. The blob feature in XTALVIEW has been applied to limit the electron density display within 1.5 Å of the residues. (c) Stereoview of the protease binding pocket of molecule A.

10 μL onto a C18 reverse-phase column (Vydac, 0.18 mm × 150 mm) using an LC Packings (Sunnyvale, CA) autosampler and pumps. The LC gradient from 2 to 60% solution B [85% ACN, 5% 2-propanol (IPA), 9.9% ddH_2O, and 0.1% TFA] was used to elute the peptides from the column at a rate of 1.0 μL/min. The column effluent was mixed in a "T" junction (Upchurch Scientific, Oak Harbor, WA) as described by Rosas-Acosta and co-workers (*55*) with a solution of α-cyano-4-hydroxycinnamic acid (CHCA, 7.5 mg/mL) (Sigma Aldrich) at a rate of 1.5 μL/min. CHCA was prepared in a 12:7:1 ACN/ddH_2O/IPA solution with 10 mM ammonium dihydrogen phosphate and doped with 50 fmol/μL bradykinin fragment 2-9 and 150 fmol/μL adrenocorticotropic hormone fragment 18-39 used as internal mass calibrants. The resulting solution was directly spotted onto MALDI plates using a robotic spotter (ProBot, LC Packings). Similar configurations for LC and other separation modes have been reported using the ProBot for fraction collection (*55, 56*). The LC fractions were spotted every 6 s. Two MALDI plates were used per injection, each plate containing 624 spots. The resulting LC separations were interrogated using a 4700 Proteomics Analyzer (Applied Biosystems) in both MALDI-MS and MS/MS acquisition modes. MALDI-MS data for each LC fraction were obtained using the reflectron detector in positive mode (700–4500 Da, 2100 Da focus mass) with internal mass calibration. Tandem MS data were acquired for each chromatographic peak using the following precursor selection: signal-to-noise threshold, 50; 12 precursors/fraction; 150 ppm fraction-to-fraction mass tolerance; chromatographic peak width, six fractions; and 3600 laser shots. Autolytic peptides were identified using both the MS-NonSpecific tool available on Protein Prospector (http://prospector.ucsf.edu/prospector/4.0.8/mshome.htm) and the corresponding tandem MS data.

N-Terminal Amino Acid Sequence Analysis. After SDS−PAGE, the protein sample was electroblotted onto a polyvinylidene fluoride (PVDF) membrane and visualized via Coomassie brilliant blue staining. The proteins were excised from the PVDF membrane and analyzed with a Hewlett-Packard G1005A Automated Protein Sequencer at the Protein Chemistry Laboratory (Texas A&M University).

RESULTS AND DISCUSSION

htrA2 Is Required for Mouse Virulence. To improve our understanding of the physiological function of HtrA homologues, deletion of the three genes (*htrA1*, *htrA2*, and *htrA3*) was achieved in *Mtb* using specialized transduction (*39*).

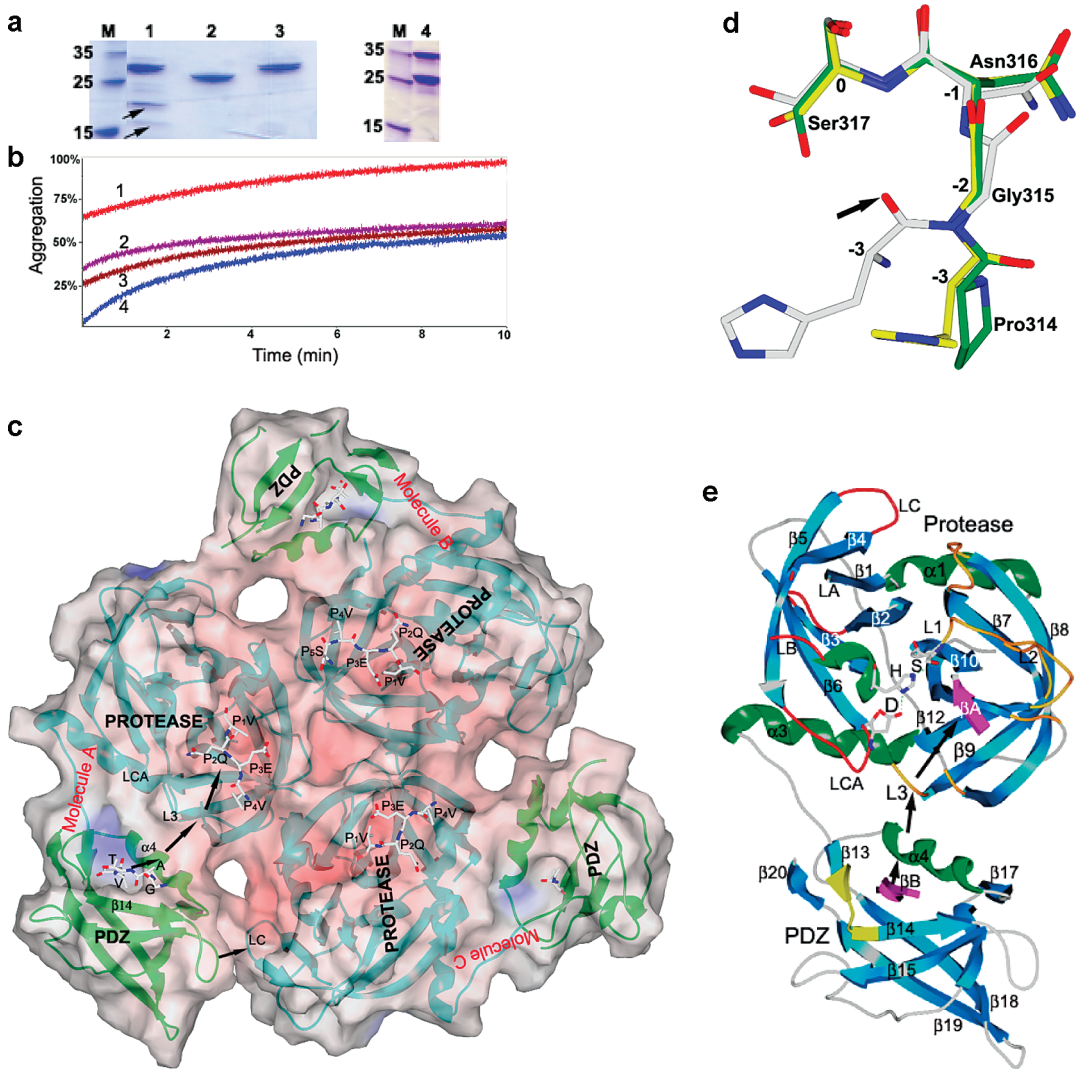

FIGURE 2: (a) Proteolytic activity against β-casein resolved by SDS−PAGE (4 to 20% gradient gel). Lane 1 shows the mHtrA2 enzyme tested against β-casein at 37 °C. Lane 2 (β-casein only) and lane 3 (mHtrA2 only) are controls at 37 °C. Lane 4 shows the S317A mutant of Δtm-HtrA2 tested against β-casein at 37 °C. Specific mHtrA2-generated cleavage products of β-casein are indicated with arrows. The 32 kDa mHtrA2 is an autoproteolytic product of Δtm-HtrA2, and the S317A mutant of Δtm-HtrA2 is inactive. (b) Suppression of the aggregation of CS by mHtrA2, Δtm-S317A-HtrA2, and mHtrA2-PDZ. Pig heart CS denatured in 6 M guanidinium hydrochloride was diluted in 10 mM Tris buffer and incubated at 25 °C with HtrA2 [CS only (1), 4:1 mHtrA2:CS ratio (2), 4:1 Δtm-S317A-HtrA2:CS ratio (4), and 10 kDa PDZ product of the 4:1 mHtrA2:CS ratio (3)]. The aggregation of CS was monitored for 10 min by measuring the apparent light scattering absorbance at 320 nm. (c) Top view of the mHtrA2 trimer. The surface is color-coded according to its electrostatic potential. The autoproteolytic P_4V-P_3E-P_2Q-P_1V peptide fragments covalently bound to the protease domain (blue ribbon) of each subunit are shown as sticks. Another autoproteolytic tetrapeptide (GATV) binds to the PDZ domain (green ribbon). (d) Comparison of the oxyanion hole of mHtrA2 (green) with that of an inactive DegS (gray; PDB entry 1SOT) and active DegS (yellow; PDB entry 1SOZ). The arrow indicates the carbonyl oxygen atom of residue −3 in the inactive DegS. In contrast to DegS, the proline residue at the −3 position of mHtrA2 forms an unblocked oxyanion hole. (e) Ribbon diagram of molecule A of the mHtrA2 trimer. All secondary structure elements and active site loops are labeled. The catalytic triad is shown as a stick model. The autoproteolytic products βA and βB (colored magenta) bind to the protease and PDZ domains, respectively. The carboxyl terminus of the βB tetrapeptide interacts with β13−β14 loop (colored yellow) of the PDZ domain. Parts of loops L3, LA, and L2 are disordered. β-Strands of the protomer are colored cyan and helices green. Loops LA, LB, LC, and LCA are colored red; loops L1−L3 are colored golden yellow and other loops gray. The arrow indicates the interaction between the PDZ and protease domain.

Successful deletions of both *htrA2* and *htrA3* were independently generated in *Mtb*, creating two mutant strains. In parallel experiments, the generation of the Δ*htrA1* mutant could not be obtained, suggesting that *htrA1* may be essential. In addition, Sassetti et al. (*57*) have identified *htrA1* as a gene that could not be disrupted in *Mtb* using the transposon site hybridization method.

To analyze the roles that the two nonessential genes play in the virulence of *Mtb*, C57BL/6 mice were infected with these mutants. The Δ*htrA2* strain revealed a modest but significant increased time-to-death phenotype compared to the wild type or the complemented mutant (297, 245, and 252 days, respectively; $p < 0.01$) (Figure 3a). This result was confirmed with a second experiment in which mice infected with the mutant strain had a longer mean survival time than mice infected with the wild-type strain (313 and 201 days, respectively; $p < 0.01$) (Figure S1 of the Supporting Information). In contrast, the Δ*htrA3* deletion had no effect on the mean survival time of mice and no other detectable phenotype (data not shown). To further analyze

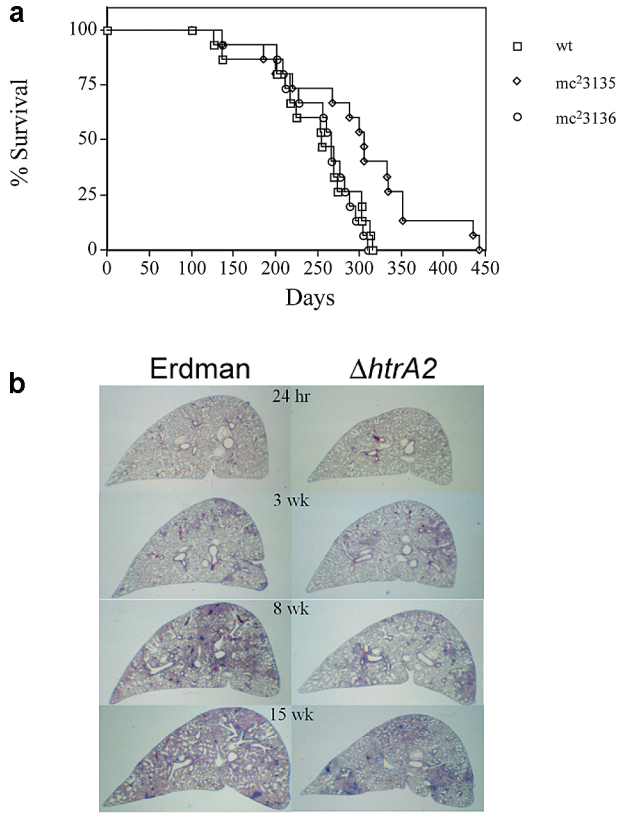

FIGURE 3: (a) Survival of C57BL/6 mice infected with wild-type *Mtb* (wt), mutant Δ*htrA2* (mc²3135), and complemented (mc²3136) strains. A significant difference in survival between the mutant strain and the complemented and wild-type strains is detected at $p < 0.01$. (b) Histopathology of lungs from mice infected with wild-type *Mtb* (*M. tuberculosis* Erdman strain) and Δ*htrA2* (mc²3135). At various time points after infection (24 h and 3, 8, and 15 weeks), lungs were fixed with 10% buffered formalin and stained with hematoxylin and eosin. Note that the number of lesions for each strain is comparable at the early time points but that the wild-type lesions have become confluent and occupy a larger proportion of the lung cross section at the later time points.

virulence, growth kinetics and pathology following mouse infections were examined. While no significant differences in CFU counts were observed 24 h or 3, 8, and 15 weeks after infection (Figure S2 of the Supporting Information), histopathological analyses did reveal differences consistent with the longer survival times of the *htrA2* deletion. At week 8, the lungs from mice infected with the wild-type strain exhibited more extensive lesions than lungs of the Δ*htrA2* infected group containing a large number of foamy macrophages filled with *Mtb* (Figure 3b). In contrast, lungs from Δ*htrA2* mutant-infected mice exhibited smaller lesions with fewer foam cells and contained fewer visible bacilli. By week 15, the number of lung lesions and the extent of pathology increased for both groups. However, the lungs from mice infected with the wild type still demonstrated larger lesions, many of which were confluent compared to the lungs of mutant-infected mice. Granulomas were present in livers and spleens at all time points, and there were also more extensive lesions in the animals infected with the wild-type strain (Figure 3b). The decreased extent of pathology thus correlated with longer survival times. These results demonstrate that *htrA2* is required for full virulence of *Mtb* in mice.

The htrA2 Gene Encodes a Serine Protease with Chaperone Activity. To further define the functional role of HtrA2 in *Mtb*, biochemical and structural characterization was performed. We have constructed and analyzed an HtrA2 variant lacking the N-terminal cytoplasmic region and its transmembrane segment. This truncated form of *Mtb*-HtrA2 (residues 125–464, designated Δtm-HtrA2) was expressed in *E. coli* and purified. While the predicted molecular mass of the recombinant protein was 37 kDa (corresponding to residues 125–464 of HtrA2 and 31 vector-derived amino acids, including N- and C-terminal His_6 tags), analysis of the molecular mass based on SDS−PAGE of the protein expressed in *E. coli* showed that the soluble recombinant protein had a mass of approximately 32 kDa. N-Terminal amino acid sequencing showed that the start of this 32 kDa protein was Ala149-Asn150-Met151-Pro152-Pro153, indicating autocleavage between Ala148 and Ala149. The 32 kDa autoproteolytic product of Δtm-HtrA2 exists as a trimer in solution [from size exclusion chromatography (data not shown)] and was shown to possess proteolytic activity against β-casein at 37 °C, generating at least two fragments (~10 and ~16 kDa) of casein (Figure 2a). The length of the degraded product from β-casein indicates that it is an endoprotease as observed for other HtrA enzymes (*7, 9, 10*). To demonstrate that this was a serine protease, we generated the S317A mutant of Δtm-HtrA2, which exhibited neither autoproteolytic nor proteolytic activity when tested against β-casein.

In addition to the serine protease activity, the HtrA2 of *Mtb* also possesses chaperone activity similar to that of HtrA of *Thermotoga maritima* (*52*). The chaperone activity of recombinant mHtrA2 and that of the S317A mutant of Δtm-HtrA2 were measured with a pig heart citrate synthase assay (*52–54*). The S317A mutant of Δtm-HtrA2 exhibited 37% inhibition of CS aggregation, while mHtrA2 exhibited 34% inhibition (Figure 2b). However, the percentage of inhibition is significantly low compared to that of an HtrA homologue from *T. maritima*, which exhibited more than 80% activity at the same molar ratio (*52*).

A second strongly expressed protein band was observed during purification, with a molecular mass of approximately 10 kDa (named mHtrA2-PDZ in Experimental Procedures). This product eluted as a monomer via size exclusion chromatography. N-Terminal amino acid sequencing of this band yielded a sequence within the HtrA2 protein starting from Ser378, the result of an autoproteolytic cleavage between Ala377 and Ser378. The 10 kDa band was not present in the S317A mutant preparation. On the basis of the crystal structure reported in the latter part of this work, Ala377 is the start of the 10 kDa PDZ domain. The cleaved PDZ domain has not been observed in any other HtrA homologues, including *E. coli*'s DegP and DegS. Furthermore, a construct with just two PDZ domains of *E. coli* DegP exhibited no chaperone activity (*8*). In contrast, the purified 10 kDa PDZ product of *Mtb*-HtrA2 exhibited chaperone-like activity similar to that of mHtrA2 (Figure 2b).

The Crystal Structure of HtrA2 Indicates a Possible Autoregulatory Mechanism. To provide further insight into the molecular mechanism of HtrA2, the crystal structure of mHtrA2 was determined at 2.0 Å resolution (Table 1). mHtrA2 forms trimers in the crystal lattice, and the subunits are named molecules A, B, and C, as shown in Figure 2c. Each subunit is composed of an N-terminal protease domain

(residues 149−364) and a C-terminal PDZ domain (residues 376−464). The three protease domains form the central core of the trimer, and the PDZ domains extend to the periphery. Similar to other serine proteases, the protease domain of each subunit has two perpendicular β-barrel lobes ($\beta1-\beta6$ and $\beta7-\beta12$) with a C-terminal helix ($\alpha3$). Loops L1 ($\beta9-\beta10$ connection), L2 ($\beta11-\beta12$), L3 ($\beta8-\beta9$), LA ($\beta1-\beta2$), LB ($\beta3-\beta4$), LC ($\beta4-\beta5$), and LCA ($\beta5-\beta6$) are defined according to the previously used nomenclature of serine proteases (Figure 2e). Interactions between the subunits of the trimer are formed exclusively by residues of the $\beta7$ and $\beta8$ strands of the serine protease domains. Although the PDZ domains make no significant interactions with their neighboring subunits, they are positioned close to the protease−protease interfaces of the trimer. The closest distance between the LC loop of the protease domain and the PDZ domain of the neighboring subunit is 4 Å. When this is taken into account, even a small change in the position of the PDZ domain would allow its $\beta14-\beta15$ loop to interact with loop LC of the neighboring protease domain and may even change the properties of the substrate binding pocket (Figure 2c).

The mHtrA2 trimer is similar to the previously reported *E. coli* DegP, *E. coli* DegS, and human HtrA2/OMI trimers (*5, 11, 16*). However, only *E. coli* DepP forms a hexameric assembly, a dimer of two trimers. The contacts between the two trimers are primarily made by a long and flexible loop, termed LA. In *E. coli*, this loop is 55 residues long, and it has been shown to block the active sites of each subunit in the adjacent trimer (*5*). These results led the authors to suggest that DegP acts as chaperone at low temperatures when the loop is blocking the protease active site, and at elevated temperatures, its protease activity is turned on via a conformational change in the loop. Previous studies have also suggested a similar mechanism of regulation for the HtrA homologue from *T. maritima* which also contains the long LA loop (*52*). In contrast, the LA loop of mHtrA2 (residues 150–155) is only six residues in length, much too short to follow the proposed switch between distinct protease or chaperone activity (Figure 4). Therefore, mHtrA2 cannot switch between a distinct protease or chaperone oligomeric state by rearranging the protease domain loops. Furthermore, there is no evidence from the crystal lattice of any higher oligomeric state.

In human HtrA2/OMI, the PDZ domain inhibits its proteolytic activity by packing directly onto its active site (*16*). In contrast, the Ser317-His197-Asp236 triad residues in each subunit of *Mtb*-HtrA2 are situated in the center of the protease domain and are freely accessible to solvent (Figure 2c). The imidazole nitrogen atom of His197 hydrogen bonds with the OH group of Ser317 (3.31 Å) of loop L1. Nδ of His197 also forms a hydrogen bond interaction (2.85 Å) with the carboxylate of Asp263 of loop LCA to complete the catalytic triad. Loop L2 (residues 291−302) is typically involved in substrate binding, forming an S1 specificity pocket near Ser317. A flexible region of loop L2 (residues 293−299) is disordered in the electron density of all three subunits. The intrasubunit interactions are similar in all three subunits; molecule A is used for the distance calculations.

In the serine protease trypsin, the NH group of Gly193 (position −2 from the active site Ser) and Ser195 [catalytic triad residue (position 0)] form the active tetrahedral oxyanion intermediate. In *E. coli* DegS, the C−O bond of the position −3 residue (position −3 from the active site Ser) points into the oxyanion hole and blocks the formation of the tetrahedral intermediate (*18*). The C-terminal tetrapeptide of the outer membrane porin binds to the PDZ domain of DegS and activates the protease domain. In the active form structure, the position −3 residue of the DegS−oxyanion hole switches its C═O group away from the NH groups to facilitate substrate binding (*17*). In contrast, *Mtb*-HtrA2 develops an active oxyanion hole formed by the Pro314-Gly315-Asn316-Ser317 residues. The position −3 residue (Pro314) imposes a steric hindrance in the *trans* conformation and facilitates the formation of the active oxyanion hole (see Figure 2d).

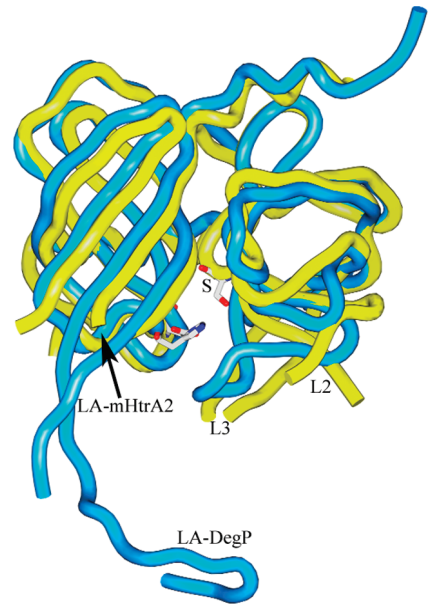

FIGURE 4: Comparison of mHtrA2's protease domain (yellow ribbon) with the protease domains of *E. coli* DegP (cyan ribbon; molecule A of PDB entry 1ky9). The catalytic triad of mHtrA2 is drawn as a stick model (active site Ser labeled). The protease domain structure is fairly conserved in both the proteins, while loop regions display significant differences. Loop LA of DegP (labeled LA-DegP) is 55 residues long and predicted to be responsible for a temperature switch. Loop LA of mHtrA2 (labeled LA-mHtrA2) is too short (residues 150–155) to follow this mechanism. Active site loops L2 and L3 of mHtrA2 are also labeled.

Interestingly, additional electron density was clearly visible in the active sites of all protease domains of the trimer (Figure 1a). This extra electron density, from an unbiased nonaveraged electron density map, was very clear and could be fitted and refined by a "VEQV" sequence (defined as P_4Val-P_3Glu-P_2Gln-P_1Val in Figure 1c). Although nearly identical electron density was observed in all three subunits of the trimer, molecule B shows additional electron density, which resembles a Ser on the N-terminal side of the peptide. We cannot rule out the possibility that other residues might extend into the solvent and may be disordered. The amino acid sequence of HtrA2 suggests that this additional electron density site belongs to a cleavage product of the recombinant protein of HtrA2 (residues V156-E157-Q158-V159). The unbiased electron density map also clearly indicates that P_1Val of the peptide is covalently linked to Oγ of the active site Ser317 (Figure 1a,c). The side chain Oγ atom of the catalytic Ser317 forms a covalent bond with the carbonyl

FIGURE 5: Summary of the LC−MALDI-MS/MS analysis of the autolytic cleavage sites of HtrA2. Arrows indicate the locations of the identified cleavage sites. We have cloned and overexpressed Δtm-HtrA2 (residues 125–472). Residues 125–148 (blue letters) were autocleaved during overexpression, yielding mature HtrA2 (mHtrA2). Apart from these, a 10 kDa PDZ domain was also observed during overexpression as a result of the autoproteolytic process. N-Terminal amino acid sequencing of mHtrA2 and the 10 kDa domain located two additional cleavage sites that are indicated by red arrows. Residues 149–364 form the protease domain of mHtrA2, and residues 376–464 form the PDZ domain. The H-D-S catalytic site residues are colored red. The tetrapeptides observed in the vicinity of the protease and PDZ binding pockets of the mHtrA2 crystal structure are highlighted in green.

carbon atom of P_1Val (1.3 Å), and its backbone oxygen atom extends into the oxyanion hole to form hydrogen bonds with the backbone nitrogen atoms of Ser317 (3.1 Å) and Gly315 (2.8 Å). The backbone of the rest of the tetrapeptide is hydrogen bonded to the protein via P_1Val N−Ser333 O (3.5 Å), P_3Glu O−I335 N (3.0 Å), and P_3Glu N−I335 O (3.4 Å) bonds. Side chain atoms of P_1Val protrude into the P_1 binding pocket formed by Ile335, Pro314, Ala334, Ile312, and Asn316. The binding of P_1Val was augmented by both hydrophobic and van der Waals interactions of these residues. Oϵ of P_2Gln forms hydrogen bonds with the side chains of Asp236 (3.1 Å) and His197 (3.1 Å) of the catalytic triad. The side chain of P_3Glu forms hydrogen bonds with the backbone oxygen atom of Ser347 (2.8 Å) and the side chain oxygen atom of Thr337 (3.0 Å), and P_4Val makes hydrophobic interactions with Val290.

These results suggest that a peptide with four (or more) residues, observed at the active site of the protease domain of each subunit, is generated by an autoproteolytic cleavage, and each protease domain of mHtrA2 is an acyl−enzyme adduct of an oligopeptide. As the binding pocket is already occupied, it is obvious that the binding of the tetrapeptide should inhibit the protease activity. In contrast, mHtrA2 exhibited clear proteolytic activity against β-casein (Figure 2a) present in the assay buffer. To correctly address this issue further, we repeated the protease assay using the enzyme derived directly from the crystals of mHtrA2. Several crystals grown under the same condition were harvested, washed extensively with the crystallization buffer, and dissolved in 10 mM Tris-HCl buffer (pH 7.5). In spite of the low yield obtained via this process, as observed in the SDS−PAGE gel, the enzyme displayed proteolytic activity, as shown in Figure S3 of the Supporting Information. Thus, the enzyme−tetrapeptide adduct observed in the crystal is, in fact, a provisional intermediate. Tri-, penta-, and tetradecapeptides have been previously observed at the catalytic sites of the acyl−enzyme adduct crystal structures of α- and γ-chymotrypsin (*58–60*), the tetra-decamer having been shown to be a potential inhibitor (*60*).

To determine the specificity of the HtrA2 protease, we monitored the autodigestion products of the dissolved crystals of mHtrA2 via LC−MALDI-MS as well as LC−ESI-MS. Linear mode MALDI-MS analysis resulted in observation of both the intact HtrA2 protein (32 kDa) and the 10 kDa PDZ fragment. Similar results were obtained from LC−ESI-MS analysis; i.e., the 32 kDa intact protein predominates until the 10 kDa fragment appears after autodigestion for 27 h. In addition, several small autolytic peptide fragments were observed in the linear mode MALDI-MS and LC−ESI-MS data. Therefore, LC−MALDI-MS was used to identity these autolytic products. Figures S4 and S5 of the Supporting

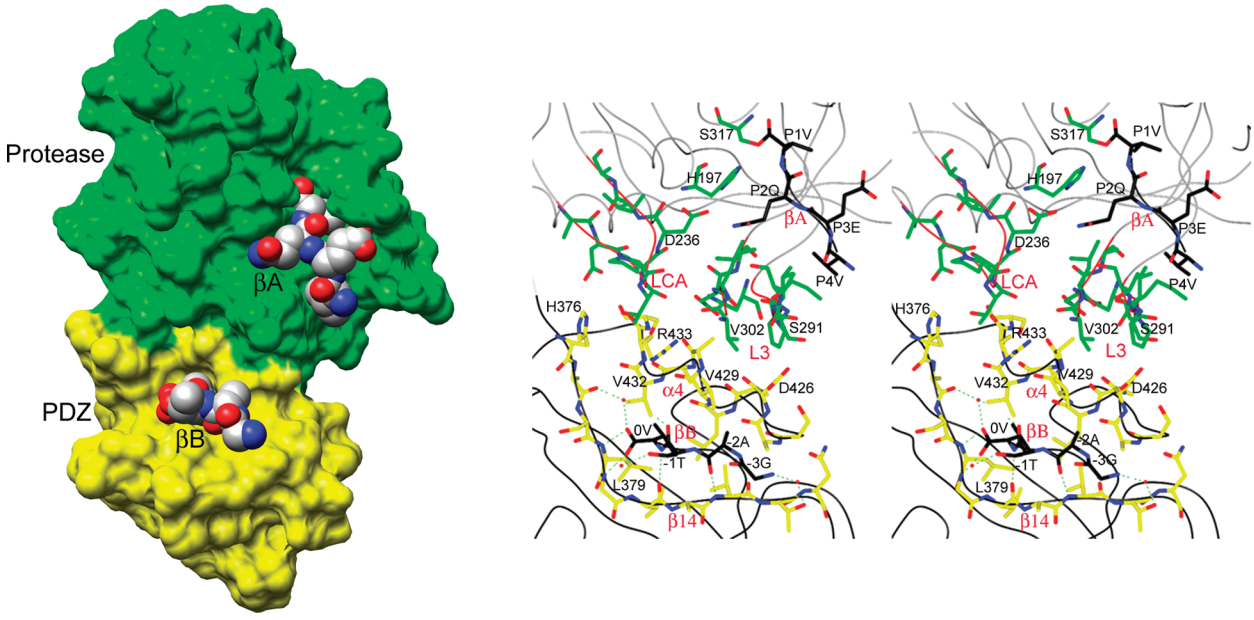

FIGURE 6: Proposed autoregulatory mechanism for mHtrA2. The autoproteolytic product GATV was bound in an extended conformation, forming an additional βB strand to β14 of the PDZ domain of mHtrA2. The side chain residues of this tetrapeptide make a network of nonbonding interactions involving α4, L3, LCA, the protease binding pocket, and the second autoproteolytic product βA. Binding of βA and βB should modulate the activity of HtrA2. The left panel shows the relative positioning of PDZ- and protease-bound tetrapeptides. The right panel (stereoview) shows the detailed interactions between the PDZ binding pocket and protease active site. The protease domain is colored green and the PDZ domain yellow.

Information show representative LC−MALDI-MS data for a single LC fraction containing a few autolytic peptides and the peptides used as internal mass calibrants. The identity of these autolytic peptides was confirmed from tandem MS analysis. For example, the tandem MS data for PPGSVEQV (*m*/*z* 812.42) shown in Figure S5B of the Supporting Information illustrate a nearly complete series of b-type fragment ions. The additional tandem MS data confirmed HtrA2 autolytic peptides observed from the LC−MALDI-MS analysis are summarized in Table S1 of the Supporting Information.

Figure 5 summarizes the results of LC−MALDI-MS/MS analysis. The analysis of the amino acid sequence at the autolytic cleavage sites clearly indicates the dominance of the Val residue with the highest propensity for autolytic attack; 18 of 40 potential cleavage sites identified by LC−MS analysis are at the carboxyl side of the Val residue. Similarly, the most important residues next to Val are Ala (six sites), Thr (five sites), Ile (five sites), Ser (four sites), and Leu (two sites). These results are consistent with the active sites of the mHtrA2 crystal structure. Interestingly, the PDZ pocket of the HtrA2 structure also displays marked complementarity to the Val residue, as described below.

The structure of the PDZ domain of *Mtb*-HtrA2 is similar to that of other bacterial PDZ domains with seven β-strands, two α-helices, and a carboxylate-binding loop formed by Ser378, Leu379, Gly380, and Val381. Surprisingly, significant electron density was also visible in the peptide-binding pocket of the PDZ domain formed by β-strand β14, the N-terminal SLGV loop, and α-helix strand α4. The additional electron density was clear only in subunit A of the trimer and could be modeled and refined by an extended tetrapeptide with the GATV sequence, which matches Gly438, Ala439, Thr440, and Val441 of HtrA2 (Figure 1b). Each protomer of the mHtrA2 structure had continuous electron density for residues 156–159 (SVEQ) and 438–441 (GATV). The LC−MS analysis of the dissolved crystals shows no evidence of any short tetrapeptides. However, the analysis did confirm the presence of an 11-amino acid peptide that ended with GATV and a nine-amino acid peptide that ended with VEQV (see Figure 5 and Table S1 of the Supporting Information). These results and the analysis of the autolytic sites suggest that the tetrapeptides observed in the crystal structure should be longer. It is possible that the N-terminal ends of these peptides are disordered in the crystal structure and are not visible in the electron density map.

The autoproteolytic product GATV binds to the PDZ domain of HtrA2 by forming an additional β-sheet (βB) to β14 through the backbone interactions typical of an antiparallel β-sheet. The C-terminus of βB is anchored by the carboxylate-binding loop of the PDZ domain. A similar type of β-augmentation was previously observed in other PDZ−peptide complexes, including DegS (*11, 14, 17*). In HtrA2, the carboxyl-terminal residue of the βB tetrapeptide [Val(0) of G(−3)A(−2)T(−1)V(0)] forms a hydrogen bond interaction with the backbone nitrogen atoms of peptide-binding pocket residues Leu379 (2.8 Å) and Gly380 (2.9 Å) (Figure 6). The carboxyl oxygen atoms of Val(0) also form a water-mediated hydrogen bond with the backbone oxygen atom of Ala377 and the backbone and side chain oxygen atoms of Thr(−1). Val(0)'s side chain is buried into the hydrophobic pocket formed by residues Val432, Val429, Leu428, and Leu379. Binding of the tetrapeptide is further stabilized by hydrogen bond interactions between Ala(−2) O and Val383 N (2.9 Å) and between Ala(−2) N and Val383 O at 3.0 Å. The backbone nitrogen of Gly(−3) forms a water-mediated hydrogen bond interaction with the side chain oxygen atom of Thr384. Interestingly, helix α4 makes a significant interaction with loop L3 of the protease domain. The side chain oxygen atom of Asp426 of α4 forms hydrogen bond interactions with the side chain oxygen atom of Ser291 of L3 (2.8 Å). Residues Val429 and Ala430 of α4 form hydrophobic interactions with Val302 of loop L3. One of the side chain nitrogens of Arg433 forms a hydrogen bond with the backbone oxygen atom of Val302 (3.5 Å). Together, the PDZ-bound tetrapeptide makes a network of nonbonded interactions with protease domain loop L3 through α4 (Figure 6). Under stressful conditions, *E. coli*'s outer membrane porin binds to the PDZ domain of DegS and activates the protease domain through "bound peptide−α4−L3−active site" interactions (*17*). Although *Mtb*-HtrA2 is active in its native form, the binding of the tetrapeptide to the PDZ domain should have an effect on the substrate specificity and might regulate the activity of its protease domain.

While the physiological consequences of the observed autocleavage are unclear, these studies indicate that the *Mtb*-HtrA2 forms an active oxyanion hole and an active protease, which might regulate itself by its autoproteolytic products. Our studies suggest that the release of HtrA2 from the membrane is more likely to be achieved by an autoproteolytic mechanism, as there is no signal peptide cleavage sequence evident at the N-terminus of the protein. Also, we illustrated the dominance of Val-specific autolytic cleavage that might play a major role in the HtrA2-associated virulence of the pathogen. The role of richness of Val and other hydrophobic residue clusters at the cleavage sites of these proteases, such as *Mtb*-HtrA2, warrants further investigation.

ACKNOWLEDGMENT

We thank Larry Dangott for numerous scientific discussions. We also thank Sudharsan Sridharan, Bing Chen, Mei Chen, Radma Mahmood, and Joanne Wang for their technical assistance; Justin McDonough for his assistance with statistical analysis; and Leslie Nicosia, Sabine Daugelat, Mary Hondalus, Michelle Larsen, Jordan Kriakov, and Sunhee Lee for their input in the editing of the manuscript.

SUPPORTING INFORMATION AVAILABLE

Survival of C57BL/6 mice infected with wild-type *Mtb* and mutant Δ*htrA2* (Figure S1), colony-forming units in the lungs, spleen, and liver of mice infected with wild-type *Mtb*, Δ*HtrA2*, and complemented strains (Figure S2), proteolytic activity of mHtrA2 protein crystals (Figure S3), mass spectrometric analysis of mHtrA2-dissolved crystals (Figures S4 and S5 and Table S1). This section also provides the primer sequence information and elaborates more on gene cloning, protein purification, gene deletion, and mouse virulence experiments. This material is available free of charge via the Internet at http://pubs.acs.org.

REFERENCES

1. Wulfing, C., and Pluckthun, A. (1994) Protein folding in the periplasm of *Escherichia coli*. *Mol. Microbiol. 12*, 685–692.

2. Arie, J. P., Sassoon, N., and Betton, J. M. (2001) Chaperone function of FkpA, a heat shock prolyl isomerase, in the periplasm of *Escherichia coli*. *Mol. Microbiol. 39*, 199–210.
3. Lazar, S. W., and Kolter, R. (1996) SurA assists the folding of *Escherichia coli* outer membrane proteins. *J. Bacteriol. 178*, 1770–1773.
4. Missiakas, D., Betton, J. M., and Raina, S. (1996) New components of protein folding in extracytoplasmic compartments of *Escherichia coli* SurA, FkpA and Skp/OmpH. *Mol. Microbiol. 21*, 871–884.
5. Krojer, T., Garrido-Franco, M., Huber, R., Ehrmann, M., and Clausen, T. (2002) Crystal structure of DegP (HtrA) reveals a new protease-chaperone machine. *Nature 416*, 455–459.
6. Swamy, K. H., Chung, C. H., and Goldberg, A. L. (1983) Isolation and characterization of protease do from *Escherichia coli*, a large serine protease containing multiple subunits. *Arch. Biochem. Biophys. 224*, 543–554.
7. Lipinska, B., Zylicz, M., and Georgopoulos, C. (1990) The HtrA (DegP) protein, essential for *Escherichia coli* survival at high temperatures, is an endopeptidase. *J. Bacteriol. 172*, 1791–1797.
8. Spiess, C., Beil, A., and Ehrmann, M. (1999) A temperature-dependent switch from chaperone to protease in a widely conserved heat shock protein. *Cell 97*, 339–347.
9. Clausen, T., Southan, C., and Ehrmann, M. (2002) The HtrA family of proteases: Implications for protein composition and cell fate. *Mol. Cell 10*, 443–455.
10. Pallen, M. J., and Wren, B. W. (1997) The HtrA family of serine proteases. *Mol. Microbiol. 26*, 209–221.
11. Doyle, D. A., Lee, A., Lewis, J., Kim, E., Sheng, M., and MacKinnon, R. (1996) Crystal structures of a complexed and peptide-free membrane protein-binding domain: Molecular basis of peptide recognition by PDZ. *Cell 85*, 1067–1076.
12. van Ham, M., and Hendriks, W. (2003) PDZ domains: Glue and guide. *Mol. Biol. Rep. 30*, 69–82.
13. Harrison, S. C. (1996) Peptide-surface association: The case of PDZ and PTB domains. *Cell 86*, 341–343.
14. Songyang, Z., Fanning, A. S., Fu, C., Xu, J., Marfatia, S. M., Chishti, A. H., Crompton, A., Chan, A. C., Anderson, J. M., and Cantley, L. C. (1997) Recognition of unique carboxyl-terminal motifs by distinct PDZ domains. *Science 275*, 73–77.
15. Schlieker, C., Mogk, A., and Bukau, B. (2004) A PDZ switch for a cellular stress response. *Cell 117*, 417–419.
16. Li, W., Srinivasula, S. M., Chai, J., Li, P., Wu, J. W., Zhang, Z., Alnemri, E. S., and Shi, Y. (2002) Structural insights into the pro-apoptotic function of mitochondrial serine protease HtrA2/Omi. *Nat. Struct. Biol. 9*, 436–441.
17. Wilken, C., Kitzing, K., Kurzbauer, R., Ehrmann, M., and Clausen, T. (2004) Crystal structure of the DegS stress sensor: How a PDZ domain recognizes misfolded protein and activates a protease. *Cell 117*, 483–494.
18. Danese, P. N., Snyder, W. B., Cosma, C. L., Davis, L. J., and Silhavy, T. J. (1995) The Cpx two-component signal transduction pathway of *Escherichia coli* regulates transcription of the gene specifying the stress-inducible periplasmic protease, DegP. *Genes Dev. 9*, 387–398.
19. Buelow, D. R., and Raivio, T. L. (2005) Cpx signal transduction is influenced by a conserved N-terminal domain in the novel inhibitor CpxP and the periplasmic protease DegP. *J. Bacteriol. 187*, 6622–6630.
20. Walsh, N. P., Alba, B. M., Bose, B., Gross, C. A., and Sauer, R. T. (2003) OMP peptide signals initiate the envelope-stress response by activating DegS protease via relief of inhibition mediated by its PDZ domain. *Cell 113*, 61–71.
21. Kadokura, H., Kawasaki, H., Yoda, K., Yamasaki, M., and Kitamoto, K. (2001) Efficient export of alkaline phosphatase overexpressed from a multicopy plasmid requires degP, a gene encoding a periplasmic protease of *Escherichia coli*. *J. Gen. Appl. Microbiol. 47*, 133–141.
22. Guigueno, A., Belin, P., and Boquet, P. L. (1997) Defective export in *Escherichia coli* caused by DsbA′-PhoA hybrid proteins whose DsbA′ domain cannot fold into a conformation resistant to periplasmic proteases. *J. Bacteriol. 179*, 3260–3269.
23. Betton, J. M., Boscus, D., Missiakas, D., Raina, S., and Hofnung, M. (1996) Probing the structural role of an $\alpha\beta$ loop of maltose-binding protein by mutagenesis: Heat-shock induction by loop variants of the maltose-binding protein that form periplasmic inclusion bodies. *J. Mol. Biol. 262*, 140–150.
24. Zeth, K. (2004) Structural analysis of DegS, a stress sensor of the bacterial periplasm. *FEBS Lett. 569*, 351–358.
25. Cortes, G., de Astorza, B., Benedi, V. J., and Alberti, S. (2002) Role of the htrA gene in *Klebsiella pneumoniae* virulence. *Infect. Immun. 70*, 4772–4776.
26. Jones, C. H., Bolken, T. C., Jones, K. F., Zeller, G. O., and Hruby, D. E. (2001) Conserved DegP protease in Gram-positive bacteria is essential for thermal and oxidative tolerance and full virulence in *Streptococcus pyogenes*. *Infect. Immun. 69*, 5538–5545.
27. Phillips, R. W., Elzer, P. H., and Roop, R. M. (1995) A *Brucella melitensis* high temperature requirement A (htrA) deletion mutant demonstrates a stress response defective phenotype in vitro and transient attenuation in the BALB/c mouse model. *Microb. Pathog. 19*, 227–284.
28. Williams, K., Oyston, P. C., Dorrell, N., Li, S., Titball, R. W., and Wren, B. W. (2000) Investigation into the role of the serine protease HtrA in *Yersinia pestis* pathogenesis. *FEMS Microbiol. Lett. 186*, 281–286.
29. Fu, L. M., and Fu-Liu, C. S. (2002) Is *Mycobacterium tuberculosis* a closer relative to Gram-positive or Gram-negative bacterial pathogens? *Tuberculosis 82*, 85–90.
30. Xiong, Y., Chalmers, M. J., Gao, F. P., Cross, T. A., and Marshall, A. G. (2005) Identification of *Mycobacterium tuberculosis* H37Rv integral membrane proteins by one-dimensional gel electrophoresis and liquid chromatography electrospray ionization tandem mass spectrometry. *J. Proteome Res. 4*, 855–861.
31. Skeiky, Y. A., Lodes, M. J., Guderian, J. A., Mohamath, R., Bement, T., Alderson, M. R., and Reed, S. G. (1999) Cloning, expression, and immunological evaluation of two putative secreted serine protease antigens of *Mycobacterium tuberculosis*. *Infect. Immun. 67*, 3998–4007.
32. Downing, K. J., McAdam, R. A., and Mizrahi, V. (1999) *Staphylococcus aureus* nuclease is a useful secretion reporter for mycobacteria. *Gene 239*, 293–299.
33. Braunstein, M., Griffin, T. I., Kriakov, J. I., Friedman, S. T., Grindley, N. D., and Jacobs, W. R., Jr. (2000) Identification of genes encoding exported *Mycobacterium tuberculosis* proteins using a Tn552′phoA in vitro transposition system. *J. Bacteriol. 182*, 2732–2740.
34. Zahrt, T. C., and Deretic, V. (2001) *Mycobacterium tuberculosis* signal transduction system required for persistent infections. *Proc. Natl. Acad. Sci. U.S.A. 98*, 12706–12711.
35. He, H., Hovey, R., Kane, J., Singh, V., and Zahrt, T. C. (2006) MprAB is a stress-responsive two-component system that directly regulates expression of sigma factors SigB and SigE in *Mycobacterium tuberculosis*. *J. Bacteriol. 188*, 2134–2143.
36. He, H., and Zahrt, T. C. (2005) Identification and characterization of a regulatory sequence recognized by *Mycobacterium tuberculosis* persistence regulator MprA. *J. Bacteriol. 187*, 202–212.
37. Larsen, M. H. (2000) *Some common methods in Mycobacteria genetics* (HatfullG. F., and Jacobs, W. R., Jr., Eds.) ASM Press, Washington, DC.
38. Braunstein, M., and Bardarov, S. S., Jr. (2002) *Genetic methods for deciphering virulence determinants of Mycobacterium tuberculosis*, Vol. 358, Academic Press, New York.
39. Bardarov, S., Bardarov, S., Jr., Pavelka, M. S., Sambandamurthy, V., Larsen, M., Tufariello, J., Chan, J., Hatfull, G., and Jacobs, W. R. (2002) Specialized transduction: An efficient method for generating marked and unmarked targeted gene disruptions in *Mycobacterium tuberculosis*, *M. bovis* BCG and *M. smegmatis*. *Microbiology 148*, 3007–3017.
40. Otwinowski, Z., and Minor, W. (1997) Processing of X-ray Diffraction Data Collected in Oscillation Mode. *Methods Enzymol. 276*, 307–326.
41. Hendrickson, W. A. (1991) Determination of macromolecular structures from anomalous diffraction of synchrotron radiation. *Science 254*, 51–58.
42. Sheldrick, G. M., and Gould, R. O. (1995) Structure solution by iterative peaklist optimization and tangent expansion in space group P1. *Acta Crystallogr. B51*, 423–431.
43. de La Fortelle, E., and Bricogne, G. (1997) Maximum-likelihood heavy-atom parameter refinement for multiple isomorphous replacement and multiwavelength anomalous diffraction methods. *Methods Enzymol. 276*, 472–494.
44. Collaborative Computational Project Number 4 (1994) The CCP4 suite: Programs for protein crystallography. *Acta Crystallogr. 50*, 760–763.
45. Abrahams, J. P., and Leslie, A. G. (1996) Methods used in the structure determination of bovine mitochondrial F1 ATPase. *Acta Crystallogr. 52*, 30–42.

46. McRee, D. E. (1999) XtalView/Xfit: A versatile program for manipulating atomic coordinates and electron density. *J. Struct. Biol. 125*, 156–165.
47. Murshudov, G. N., Vagin, A. A., and Dodson, E. J. (1997) Refinement of macromolecular structures by the maximum-likelihood method. *Acta Crystallogr. 53*, 240–255.
48. Laskowski, R. A., MacArthur, M. W., Moss, D. S., and Thornton, J. M. (1993) PROCHECK: A program to check the stereochemical quality of protein structures. *J. Appl. Crystallogr. 26*, 283–291.
49. Laskowski, R. A., Moss, D. S., and Thornton, J. M. (1993) Main-chain bond lengths and bond angles in protein structures. *J. Mol. Biol. 231*, 1049–1067.
50. Merritt, E. A., and Murphy, M. E. (1994) Raster3D Version 2.0. A program for photorealistic molecular graphics. *Acta Crystallogr. 50*, 869–873.
51. Pettersen, E. F., Goddard, T. D., Huang, C. C., Couch, G. S., Greenblatt, D. M., Meng, E. C., and Ferrin, T. E. (2004) UCSF Chimera: A visualization system for exploratory research and analysis. *J. Comput. Chem. 25*, 1605–1612.
52. Kim, D. Y., Kim, D. R., Ha, S. C., Lokanath, N. K., Lee, C. J., Hwang, H. Y., and Kim, K. K. (2003) Crystal structure of the protease domain of a heat-shock protein HtrA from *Thermotoga maritima*. *J. Biol. Chem. 278*, 6543–6551.
53. Büchner, J., Grallert, H., and Jakob, U. (1998) Analysis of chaperone function using citrate synthase as nonnative substrate protein. *Methods Enzymol. 290*, 323–338.
54. Huston, W. M., Swedberg, J. E., Harris, J. M., Walsh, T. P., Mathews, S. A., and Timms, P. (2007) The temperature activated HtrA protease from pathogen *Chlamydia trachomatis* acts as both a chaperone and protease at 37 °C. *FEBS Lett. 581*, 3382–3386.
55. Rosas-Acosta, G., Russell, W. K., Deyrieux, A., Russell, D. H., and Wilson, V. G. (2005) A universal strategy for proteomic studies of SUMO and other ubiquitin-like modifiers. *Mol. Cell. Proteomics 4*, 56–72.
56. Williams, B. J., Russell, W. K., and Russell, D. H. (2007) Utility of CE-MS data in protein identification. *Anal. Chem. 79*, 3850–3855.
57. Sassetti, C. M., Boyd, D. H., and Rubin, E. J. (2003) Genes required for mycobacterial growth defined by high density mutagenesis. *Mol. Microbiol. 48*, 77–84.
58. Dixon, M. M., and Matthews, B. W. (1989) Is γ-chymotrypsin a tetrapeptide acyl-enzyme adduct of α-chymotrypsin? *Biochemistry 28*, 7033–7038.
59. Harel, M., Su, C. T., Frolow, F., Silman, I., and Sussman, J. L. (1991) γ-Chymotrypsin is a complex of α-chymotrypsin with its own autolysis products. *Biochemistry 30*, 5217–5225.
60. Singh, N., Jabeen, T., Sharma, S., Roy, I., Gupta, M. N., Bilgrami, S., Somvanshi, R. K., Dey, S., Perbandt, M., Betzel, C., Srinivasan, A., and Singh, T. P. (2005) Detection of native peptides as potent inhibitors of enzymes. Crystal structure of the complex formed between treated bovine α-chymotrypsin and an autocatalytically produced fragment, IIe-Val-Asn-Gly-Glu-Glu-Ala-Val-Pro-Gly-Ser-Trp-Pro-Trp, at 2.2 angstroms resolution. *FEBS J. 272*, 562–572.

BI701929M